

1     **A GENERALISED RANDOM ENCOUNTER MODEL FOR ESTIMATING**  
2                     **ANIMAL DENSITY WITH REMOTE SENSOR DATA**

3     **Running title: A generalised random encounter model for animals.**

4     **Word count:**

5     **Authors:**

6     Tim C.D. Lucas<sup>1,2,3</sup>, Elizabeth A. Moorcroft<sup>1,4,5</sup>, Robin Freeman<sup>5</sup>, Marcus J. Rowcliffe<sup>5</sup>,  
7     Kate E. Jones<sup>2,5</sup>

8     **Addresses:**

9     1 CoMPLEX, University College London, Physics Building, Gower Street, Lon-  
10    don, WC1E 6BT, UK

11    2 Centre for Biodiversity and Environment Research, Department of Genetics,  
12    Evolution and Environment, University College London, Gower Street, London,  
13    WC1E 6BT, UK

14    3 Department of Statistical Science, University College London, Gower Street,  
15    London, WC1E 6BT, UK

16    4 Department of Computer Science, University College London, Gower Street,  
17    London, WC1E 6BT, UK

18    5 Institute of Zoology, Zoological Society of London, Regents Park, London, NW1  
19    4RY, UK

20    **Corresponding authors:**

21    Kate E. Jones,  
22    Centre for Biodiversity and Environment Research,  
23    Department of Genetics, Evolution and Environment,  
24    University College London,  
25    Gower Street,  
26    London,  
27    WC1E 6BT,  
28    UK

29 kate.e.jones@ucl.ac.uk

30

31 Marcus J. Rowcliffe,

32 Institute of Zoology,

33 Zoological Society of London,

34 Regents Park,

35 London,

36 NW1 4RY,

37 UK

38 marcus.rowcliffe@ioz.ac.uk

ABSTRACT

39  
40 **1:** Wildlife monitoring technology has advanced rapidly and the use of remote  
41 sensors such as camera traps, and acoustic detectors is becoming common in both  
42 the terrestrial and marine environments. Current methods to estimate abundance  
43 or density require individual recognition of animals or knowing the distance of  
44 the animal from the sensor, which is often difficult. A method without these re-  
45 quirements, the random encounter model (REM), has been successfully applied to  
46 estimate animal densities from count data generated from camera traps. However,  
47 count data from acoustic detectors do not fit the assumptions of the REM due to  
48 the directionality of animal signals.

49 **2:** We developed a generalised REM (gREM), to estimate absolute animal density  
50 from count data from both camera traps and acoustic detectors. We derived the  
51 gREM for different combinations of sensor detection widths and animal signal  
52 widths (a measure of directionality). We tested the accuracy and precision of this  
53 model using simulations of different combinations of sensor detection widths and  
54 animal signal widths, number of captures, and models of animal movement.

55 **3:** We find that the gREM produces accurate estimates of absolute animal density  
56 for all combinations of sensor detection widths and animal signal widths. How-  
57 ever, larger sensor detection and animal signal widths were found to be more pre-  
58 cise. While the model is accurate for all capture efforts tested, the precision of the  
59 estimate increases with the number of captures. We found no effect of different  
60 animal movement models tested on the accuracy and precision of the gREM.

61 **4:** We conclude that the gREM provides an effective method to estimate absolute  
62 animal densities from remote sensor count data over a range of sensor and animal  
63 signal widths. The gREM is applicable for count data obtained in both marine and  
64 terrestrial environments, visually or acoustically (e.g., big cats, sharks, birds, bats  
65 and cetaceans). As sensors such as camera traps and acoustic detectors become  
66 more ubiquitous, the gREM will be increasingly useful for monitoring unmarked  
67 animal populations across broad spatial, temporal and taxonomic scales.

**Keywords.** acoustic detection, camera traps, marine, population monitoring, simulations, terrestrial

## INTRODUCTION

Animal population density is one of the fundamental measures needed in ecology and conservation. The density of a population has important implications for a range of issues such as sensitivity to stochastic fluctuations (Richter-Dyn & Goel, 1972; Wright & Hubbell, 1983) and risk of extinction (Purvis *et al.*, 2000). Monitoring animal population changes in response to anthropogenic pressure is becoming increasingly important as humans modify habitats and change climates as never before (Everatt *et al.*, 2014). Sensor technology, such as camera traps (Rowcliffe & Carbone, 2008; Karanth, 1995) and acoustic detectors (O’Farrell & Gannon, 1999; Clark, 1995; Acevedo & Villanueva-Rivera, 2006) are becoming increasingly used to monitor changes in animal populations (Rowcliffe & Carbone, 2008; Kessel *et al.*, 2014), as they are efficient, relatively cheap and non-invasive (Cutler & Swann, 1999), allowing for surveys over large areas and long periods. However, the problem of converting sampled count data to estimates of density remains as efforts must be made to account for detectability of the animals (Anderson, 2001).

Methods do already exist for estimating animal density but these methods often require additional information that may not be available. For example, capture-mark-recapture methods (Karanth, 1995; Trolle & Kéry, 2003; Soisalo & Cavalcanti, 2006; Trolle *et al.*, 2007; ?) require recognition of individuals, distance methods (Harris *et al.*, 2013) require an estimation of how far away individuals are from the sensor (Barlow & Taylor, 2005; Marques *et al.*, 2011). The development of the random encounter model (REM) (a modification of a gas model) enabled animal densities to be estimated from unmarked individuals of a known speed, and sensor detection parameters (Rowcliffe *et al.*, 2008). The REM method has been successfully applied to estimate animal densities from camera trap surveys (Manzo *et al.*, 2012; Zero *et al.*, 2013). However, extending the REM method to other types of sensors (for example acoustic detectors) is more problematic, because the original derivation assumes a relatively narrow sensor width (up to  $\pi/2$  radians) and that the animal is equally detectable irrespective of its heading (Rowcliffe *et al.*, 2008).

99     Whilst these restrictions are not problematic for most camera trap makes (e.g.  
100     Reconyx, Cuddeback), the REM could not be used to estimate densities from cam-  
101     era traps with a wider sensor width (e.g. canopy monitoring with fish eye lens  
102     (Brusa & Bunker, 2014)). Additionally, the REM method would not be useful in  
103     estimating densities from acoustic survey data as the acoustic detector angles are  
104     often wider than  $\pi/2$  radians. Acoustic detectors are designed for a range of di-  
105     verse tasks and environments (Kessel *et al.*, 2014), which will naturally lead to a  
106     wide range of sensor detection widths and detection distances. In addition to this,  
107     calls emitted by many animals are directional (Blumstein *et al.*, 2011) breaking the  
108     assumption of the REM method.

109     There has been a sharp rise in interest around passive acoustic detectors in re-  
110     cent years, with a 10 fold increase in publications in the decade between 2000 and  
111     2010 (Kessel *et al.*, 2014). Acoustic monitoring is being developed to study many  
112     aspects of ecology, including the interactions of animals and their environments  
113     (Blumstein *et al.*, 2011; Rogers *et al.*, 2013), the presence and relative abundances of  
114     species (Marcoux *et al.*, 2011), and biodiversity of an area (Depraetere *et al.*, 2012).

115     Acoustic data suffers from many of the problems associated with data from  
116     camera trap surveys in that individuals are often unmarked so capture-mark-  
117     recapture methods cannot be used to estimate densities. In some cases the dis-  
118     tance between the animal and the sensor is known, for example when an array of  
119     sensors and the position of the animal is estimated by triangulation (Lewis *et al.*,  
120     2007). In these situations distance-sampling methods can be applied, a method  
121     typically used for marine mammals (Rogers *et al.*, 2013). However, in many cases  
122     distance estimation is not possible, for example when single sensors are deployed,  
123     a situation typical in the majority of terrestrial acoustic surveys (Elphick, 2008;  
124     Buckland *et al.*, 2008). In these cases, only relative measures of local abundance can  
125     be calculated, and not absolute densities. This means that comparison of popula-  
126     tions between species and sites is problematic without assuming equal detectabil-  
127     ity (Schmidt, 2003; ?; Walters *et al.*, 2013). Equal detectability is unlikely because of  
128     differences in environmental conditions, sensor type, habitat, species biology.

129     In this study we create a generalised REM (gREM), as an extension to the cam-  
130     era trap model of (Rowcliffe *et al.*, 2008), to estimate absolute density from count

131 data from acoustic detectors, or camera traps, where the sensor width can vary  
 132 from 0 to  $2\pi$  radians, and the signal given from the animal can be directional. We  
 133 assessed the accuracy and precision of the gREM within a simulated environment,  
 134 by varying the sensor detection widths, animal signal widths, number of captures  
 135 and models of animal movement. We use the simulation results to recommend  
 136 best survey practice for estimating animal densities from remote sensors.

## 137 METHODS

138 **Analytical Model.** The REM presented by Rowcliffe *et al.* (2008) adapts the gas  
 139 model to model count data from camera trap surveys. The REM is derived assum-  
 140 ing a stationary sensor with a detection width less than  $\pi/2$  radians. However, in  
 141 order to apply this approach more generally, and in particular to acoustic detec-  
 142 tors, we need both to relax the constraint on sensor detection width, and allow  
 143 for animals with directional signals. Consequently, we derive the gREM for any  
 144 detection width,  $\theta$ , between 0 and  $2\pi$  with a detection distance  $r$  giving a circular  
 145 sector within which animals can be captured (the detection zone)(Figure 1). Ad-  
 146 ditionally, we model the animal as having an associated signal width  $\alpha$  between  
 147 0 and  $2\pi$ (Figure 1, see Appendix S1 for a list of symbols). We start deriving the  
 148 gREM with the simplest situation, the gas model where  $\theta = 2\pi$  and  $\alpha = 2\pi$ .

149 *Gas Model.* Following Yapp (1956), we derive the gas model where sensors can  
 150 capture animals in any direction and animal's signal is detectable from any direction( $\theta =$   
 151  $2\pi$  and  $\alpha = 2\pi$ ). We assume that animals are in a homogeneous environment, and  
 152 move in straight lines of random direction with velocity  $v$ . We allow that our sta-  
 153 tionary sensor can capture animals at a detection distance  $r$  and that if an animal  
 154 moves within this detection zone they are captured with a probability of one, while  
 155 animals outside the zone are never captured.

156 In order to derive animal density, we need to consider relative velocity from  
 157 the reference frame of the animals. Conceptually, this requires us to imagine that  
 158 all animals are stationary and randomly distributed in space, while the sensor  
 159 moves with velocity  $v$ . If we calculate the area covered by the sensor during the  
 160 survey period we can estimate the number of animals the sensor should capture.  
 161 As a circle moving across a plane, the area covered by the sensor per unit time is

162  $2rv$ . The number of expected captures,  $z$ , for a survey period of  $t$ , with an animal  
163 density of  $D$  is  $z = 2rvtD$ . To estimate the density, we rearrange to get  $D = z/2rvt$ .

164 *gREM derivations for different detection and signal widths.* Different combinations of  
165  $\theta$  and  $\alpha$  would be expected to occur (e.g., sensors have different detection widths  
166 and animals have different signal widths). For different combinations  $\theta$  and  $\alpha$ , the  
167 area covered per unit time is no longer given by  $2rv$ . Instead of the size of the  
168 sensor detection zone having a diameter of  $2r$ , the size changes with the approach  
169 angle between the sensor and the animal. For any given signal width and detec-  
170 tor width and depending on the angle that the animal approaches the sensor, the  
171 width of the area within which an animal can be detected is called the profile,  $p$ .  
172 The size of the profile (averaged across all approach angles) is defined as the aver-  
173 age profile  $\bar{p}$ . However, different combinations of  $\theta$  and  $\alpha$  need different equations  
174 to calculate  $\bar{p}$ .

175 We have identified the parameter space for the combinations of  $\theta$  and  $\alpha$  for  
176 which the derivation of the equations are the same (defined as sub-models in the  
177 gREM) (Figure 2). For example, the gas model becomes the simplest gREM sub-  
178 model (upper right in Figure 2) and the REM from Rowcliffe *et al.* (2008) is another  
179 gREM sub-model where  $\theta < \pi/2$  and  $\alpha = 2\pi$ . We derive one gREM sub-model SE2  
180 as an example below, where  $2\pi - \alpha/2 < \theta < 2\pi$ ,  $0 < \alpha < \pi$  (see Appendix S2 for  
181 other gREM sub-models).

182 *Example derivation of SE2.* In order to calculate  $\bar{p}$ , we have to integrate over the  
183 focal angle,  $x_1$  (Figure 3a). This is the angle taken from the centre line of the sensor.  
184 Other focal angles are possible ( $x_2, x_3, x_4$ ) and are used in other gREM sub-models  
185 (see Appendix S2). As the size of the profile depends on the approach angle, we  
186 present the derivation across all approach angles. When the sensor is directly  
187 approaching the animal  $x_1 = \pi/2$ .

188 Starting from  $x_1 = \pi/2$  until  $\theta/2 + \pi/2 - \alpha/2$ , the size of the profile is  $2r \sin \alpha/2$   
189 (Figure 3b). During this first interval, the size of  $\alpha$  limits the width of the profile.  
190 When the animal reaches  $x_1 = \theta/2 + \pi/2 - \alpha/2$  (Figure 3c), the size of the profile is  
191  $r \sin(\alpha/2) + r \cos(x_1 - \theta/2)$  and the size of  $\theta$  and  $\alpha$  both limit the width of the profile

(Figure 3c). Finally, at  $x_1 = 5\pi/2 - \theta/2 - \alpha/2$  until  $x_1 = 3\pi/2$ , the width of the profile is again  $2r \sin \alpha/2$  (Figure 3d) and the size of  $\alpha$  again limits the width of the profile.

The profile width  $p$  for  $\pi$  radians of rotation (from directly towards the sensor to directly behind the sensor) is completely characterised by the three intervals (Figure 3b–3d). Average profile width  $\bar{p}$  is calculated by integrating these profiles over their appropriate intervals of  $x_1$  and dividing by  $\pi$  which gives

$$\bar{p} = \frac{1}{\pi} \left( \int_{\frac{\pi}{2}}^{\frac{\pi}{2} + \frac{\theta}{2} - \frac{\alpha}{2}} 2r \sin \frac{\alpha}{2} dx_1 + \int_{\frac{\pi}{2} + \frac{\theta}{2} - \frac{\alpha}{2}}^{\frac{5\pi}{2} - \frac{\theta}{2} - \frac{\alpha}{2}} r \sin \frac{\alpha}{2} + r \cos \left( x_1 - \frac{\theta}{2} \right) dx_1 + \int_{\frac{5\pi}{2} - \frac{\theta}{2} - \frac{\alpha}{2}}^{\frac{3\pi}{2}} 2r \sin \frac{\alpha}{2} dx_1 \right) \quad \text{eqn 1}$$

$$= \frac{r}{\pi} \left( \theta \sin \frac{\alpha}{2} - \cos \frac{\alpha}{2} + \cos \left( \frac{\alpha}{2} + \theta \right) \right) \quad \text{eqn 2}$$

We then use this expression to calculate density

$$D = z/vt\bar{p}. \quad \text{eqn 3}$$

Rather than having one equation that describes  $\bar{p}$  globally, the gREM must be split into submodels due to discontinuous changes in  $p$  as  $\alpha$  and  $\beta$  change. These discontinuities can occur for a number of reasons such as a profile switching between being limited by  $\alpha$  and  $\theta$ , the difference between very small profiles and profiles of size zero and the fact that the width of a sector stops increasing once the central angle reaches  $\pi$  radians (i.e., a semi circle is just as wide as a full circle.)

As a visual example, if  $\alpha$  is small, there is an interval between Fig. 3c and 3d where the ‘blind spot’ would prevent animals being detected at all giving  $p = 0$ . This would require an extra integral in our equation as simply putting our small value of  $\alpha$  into eqn 1 would not give us this integral of  $p = 0$ .

gREM submodel specifications were done by hand, and the integration was done using SymPy (SymPy Development Team, 2014) in Python (Appendix S3). The gREM submodels were checked by confirming that: (1) submodels adjacent in parameter space were equal at the boundary between them; (2) submodels that border  $\alpha = 0$  had  $p = 0$  when  $\alpha = 0$ ; (3) average profile widths  $\bar{p}$  were between 0 and  $2r$  and; (4) each integral, divided by the range of angles that it was integrated



over, was between 0 and  $2r$ . The scripts for these tests are included in Appendix S3 and the R (R Development Core Team, 2010) implementation of the gREM is given in Appendix S4.

**Simulation Model.** We tested the accuracy and precision of the gREM by developing a spatially explicit simulation of the interaction of sensors and animals using different combinations of sensor detection widths, animal signal widths, number of captures, and models of animal movement. 100 simulations were run where each consisted of a 7.5 km by 7.5 km square with periodic boundaries. A stationary sensor of radius  $r$  was set up in the exact centre of each simulation, covering 7 sensor detection widths  $\theta$  between 0 and  $2\pi$  ( $2/9\pi, 4/9\pi, 6/9\pi, 8/9\pi, 10/9\pi, 14/9\pi, 2\pi$ ). Each simulation was populated with a density of 70 animals  $\text{km}^{-2}$ , calculated from the equation in Damuth (1981) as the expected density of mammals of weighing 1 g. This density therefore represents a reasonable estimate of density of individuals, given that the smallest mammal is around 2 g (Jones *et al.*, 2009). A total of 3937 individuals per simulation were created which were placed randomly at the start of the simulation. Individuals were assigned 11 signal widths  $\alpha$  between 0 and  $\pi$  ( $1/11\pi, 2/11\pi, 3/11\pi, 4/11\pi, 5/11\pi, 6/11\pi, 7/11\pi, 8/11\pi, 9/11\pi, 10/11\pi, \pi$ ).

Each simulation lasted for  $N$  steps (14400) of duration  $T$  (15 minutes) giving a total duration of 150 days. The individuals moved within each step with a distance  $d$ , with an average speed,  $v$ .  $d$ , was sampled from a normal distribution with mean distance,  $\mu_d = vT$ , and standard deviation  $\sigma_d = vT/10$ . An average speed,  $v = 40 \text{ km days}^{-1}$ , was chosen as this is the largest day range of terrestrial animals (Carbone *et al.*, 2005), and represents the upper limit of realistic speeds. At the end step, individuals were allowed to either remain stationary for a time step (with a given probability,  $S$ ), or change direction (in a uniform distribution with a maximum angle,  $A$ ) between 0 and  $\pi$ . This resulted in 7 different movement models where: (1) simple movement, where  $S$  and  $A = 0$ ; (2) stop-start movement, where (i)  $S = 0.25, A = 0$ , (ii)  $S = 0.5, A = 0$ , (iii)  $S = 0.75, A = 0$ ; (3) random walk movement, where (i)  $S = 0, A = \pi/3$ , (ii)  $S = 0, A = 2\pi/3$ , (iii)  $S = 0, A = \pi$ . Individuals were counted as they moved in and out of the detection zone of the sensor per simulation.

We calculated the estimated animal density from the gREM by summing the number of captures per simulation and inputting these values into the correct gREM submodel. gREM accuracy was determined by comparing the density in the simulation with the estimated density. High accuracy is indicated by the mean difference between the estimated and actual values not being significantly different from zero (Wilcoxon signed-rank test). gREM precision was determined by the standard deviation of estimated densities. We used this method to compare the accuracy and precision of all the gREM submodels. As these submodels are derived for different combinations of  $\alpha$  and  $\theta$ , the accuracy and precision of the submodels was used to determine the impact of different values of  $\alpha$  and  $\theta$ .

The influence of the number of captures and animal movement models on accuracy and precision was investigated using 4 different gREM submodels representative of the range  $\alpha$  and  $\theta$  values (submodels NW1, SW1, NE1, and SE3, Figure 2). Using these four submodels, we calculated how long the simulation needed to run to generate a range of different capture numbers (from 10 to 100 captures in 10 unit intervals), and estimated animal density. These estimated densities were compared to the real density to assess the impact on the accuracy and precision of the gREM. The gREM assumes that individuals move continuously with straight-line movement (simple movement model) and we therefore assessed the impact of breaking the gREM assumptions. We used the four submodels to compare the accuracy and precision of a simple movement model, stop-start movement models and random walk movement models.

## RESULTS

**Analytical model.** The equation for  $\bar{p}$  has been newly derived for each submodel in the gREM, except for the gas model and REM which have been calculated previously. However, many models, although derived separately, have the same expression for  $\bar{p}$ . Figure 4 shows the expression for  $\bar{p}$  in each case. The general equation for density, using the correct expression for  $\bar{p}$  is then substituted into eqn 3. Although more thorough checks are performed in Appendix S3, it can be seen that all adjacent expressions in Figure 4 are equal when expressions for the boundaries between them are substituted in.

278 **Simulation model.**

279 *gREM submodels.* All gREM submodels showed a high accuracy, i.e., the mean dif-  
 280 ference between the estimated and actual values was not significantly different  
 281 from zero across all models, corrected for multiple tests (all gREM sub models  
 282 Wilcoxon signed-rank test,  $p > 0.002$ )(Figure 5). However, the precision of the sub-  
 283 models do vary, where the gas model is the most precise and the SW7 sub model  
 284 the least precise, having the smallest and the largest interquartile range, respec-  
 285 tively (Figure 5). The standard deviation of the error between the estimated and  
 286 true densities is strongly related to both the sensor and signal widths (Figure 6),  
 287 such that larger widths have lower standard deviations (greater precision).

288 *Number of captures.* Within the four gREM submodels tested (NW1, SW1, SE3,  
 289 NE1), the accuracy was not affected by the number of captures, where the mean  
 290 difference between the estimated and actual values was not significantly differ-  
 291 ent from zero across all capture rates, corrected for multiple tests (all gREM sub  
 292 models Wilcoxon signed-rank test,  $p > 0.008$ )(Figure 7). However, the precision  
 293 was dependent on the number of captures across all four of the gREM submod-  
 294 els, where precision increases as number of captures increases (Figure 7). For all  
 295 gREM submodels, the the coefficient of variation falls to 10% at 100 captures.

296 *Movement models.* Within the four gREM submodels tested (NW1, SW1, SE3, NE1),  
 297 neither the accuracy or precision was affected by the amount of time spent sta-  
 298 tionary. The mean difference between the estimated and actual values was not  
 299 significantly different from zero for each category of stationary time (0, 0.25, 0.5  
 300 and 0.75), corrected for multiple tests (all gREM sub models Wilcoxon signed-rank  
 301 test,  $p > 0.12$ )(Figure 8a). Altering the maximum change in direction in each step  
 302 (0,  $\pi/3$ ,  $2\pi/3$ , and  $\pi$ ) did not affect the accuracy or precision of the four gREM  
 303 submodels tested (all gREM sub models Wilcoxon signed-rank test,  $p > 0.05$ )(Fig-  
 304 ure 8b).

305 DISCUSSION

306 We have developed the gREM such that it can be used to estimate density from  
 307 acoustic sensors and camera traps. This has entailed a generalisation of the gas

model and the REM in Rowcliffe *et al.* (2008) to be applicable to any combination of sensor width and signal directionality. We have used simulations to show, as a proof of principle, that these models are accurate and precise. The precision of the gREM was found to be dependent on the width of the sensor and the call, and the number of captures.

**Analytical model.** The gREM was derived for different combinations of  $\alpha$  and  $\theta$  resulting in 25 different submodels, the expression for  $\bar{p}$  are equal for many of these submodels resulting in eight different equations including the previously derived gas model and REM. These submodels were tested for consistency with adjacent expressions being equal at their boundaries. These new submodels will allow researchers to evaluate the absolute density of animals that have previously been difficult to study, such as bats (Clement & Castleberry, 2013), with noninvasive methods such as remote sensors. The gREM allows the data from acoustic detectors to be used where an animal has a directional calls, this could be used for a range of animals including songbirds (Blumstein *et al.*, 2011), and dolphins (Lammers & Au, 2003).

There are a number of possible extensions to the gREM which could be developed in the future. The original gas model was formulated for the case where both subjects, either animal and detector, or animal and animal, are moving (Hutchinson & Waser, 2007). Indeed any of the models with animals that are equally detectable in all directions ( $\alpha = 2\pi$ ) can be trivially expanded for moving by substituting the sum of the average animal velocity and the sensor velocity for  $v$  as used here. However, when the animal has a directional call, as seen in both terrestrial and aquatic environments (Lammers & Au, 2003; Blumstein *et al.*, 2011), the extension becomes less simple. The approach would be to calculate again the mean profile width. However, for each angle of approach, one would have to average the profile width for an animal facing in any direction (i.e. not necessarily moving towards the sensor) weighted by the relative velocity of that direction. There are a number of situations where a moving detector and animal could occur, e.g. an acoustic detector towed from a boat when studying porpoises (Kimura *et al.*, 2014) or surveying bats from a moving car (Ahlen & Baagøe, 1999; ?).

339 An interesting but unstudied problem is edge effects caused by trigger delays  
340 (the delay between sensing an animal and attempting to record the encounter)  
341 (Rovero *et al.*, 2013) and time expansion acoustic detectors which repeatedly turn  
342 on an off during sampling (Ahlen & Baagøe, 1999). Both of these have potential  
343 biases as animals can move through the detection zone without being detected.  
344 The models herein are formulated assuming constant surveillance and so the error  
345 created by switching the sensor on and off quickly becomes negligible if the sensor  
346 is on for extended periods of time. For example, if it takes longer for the recording  
347 device to be switched on than the length of some animal calls there could be a  
348 systematic underestimation of density.

349 **Accuracy and Precision.** Based on our simulations we believe that the gREM has  
350 the potential to produce accurate estimates for many different species, using ei-  
351 ther camera traps or acoustic detectors. However the precision of the gREM dif-  
352 fered between submodels. For example, when the sensor and signal width were  
353 smaller than the precision of the model was reduced, so when choosing a sensor  
354 for use in a gREM study the detection width should be maximised, and if the study  
355 species has a narrow signal directionality other aspects of the study protocol, such  
356 as length of the survey, should be used to compensate.

357 The precision of the gREM is greatly affected by the number of captures that are  
358 collected, the coefficient of variation falls dramatically between 10 and 60 captures  
359 and then after this continues to slowly reduce. At 100 captures the submodels  
360 reach 10% coefficient of variation, considered to a very good level of precision  
361 (Thomas & Marques, 2012). Many current studies do not reach this level of pre-  
362 cision, with most studies reporting coefficient of variations greater than the 10%  
363 level (O'Brien *et al.*, 2003; Proctor *et al.*, 2010; Foster & Harmsen, 2012). The length  
364 of surveys in the field will need to be adjusted so that enough data can be collected  
365 to reach this level of precision. Populations of fast moving animals or populations  
366 with large densities will require less survey effort than those with slow moving or  
367 low densities.

368 The gREM was both accurate and precise for all the movement models we  
 369 tested (stop-start movement and correlated random walks). However these move-  
 370 ment models are still simple representations of true animal movement which are  
 371 dependent on multiple factors such as behavioural state and and existence of  
 372 home ranges (Smouse *et al.*, 2010). The accuracy of the gREM may be affected  
 373 by the interaction between the movement model and the size of the detection ra-  
 374 dius. We have studied a relatively long step length compared to the size of the  
 375 detection radius, and therefore the chance of catching the same animal multiple  
 376 times within a short space of time was reduced and there is little affect on the pre-  
 377 cision of the model (Figure 8b). However if the ratio of step length to detection  
 378 radius was smaller then this may decrease the precision of the model, however  
 379 this should not decrease its accuracy.

380 Although we have used simulations to validate the gREM submodels, much  
 381 more robust testing is needed. Although difficult, proper field test validation  
 382 would be required before the models could be fully trusted. The REM (Rowcliffe  
 383 *et al.*, 2008) has already been field tested, and both Rowcliffe *et al.* (2008) and Zero  
 384 *et al.* (2013) both found that the REM was an effective manner of estimating ani-  
 385 mal densities (Rowcliffe *et al.*, 2008; Zero *et al.*, 2013). In some taxa gold standard  
 386 methods of estimating animal density exist, such as capture mark recapture (Soll-  
 387 mann *et al.*, 2013). Where these gold standard exist or true numbers are known,  
 388 a simultaneous gREM study could be completed to test the accuracy under field  
 389 conditions, similar to the tests that Rowcliffe *et al.* (2008) completed with the REM.  
 390 An easier way to continue to evaluate the models is to run more extensive simula-  
 391 tions which break the assumptions of the analytical models. The main element that  
 392 cannot be analytically treated is the complex movement of real animals. There-  
 393 fore testing these methods against true animal traces, or more complex movement  
 394 models would be required.

395 Within the simulation we have assumed an equal density across the entire world,  
 396 however in a field environment the situation would be much more complex, with  
 397 additional variation coming from local changes in density between camera sites.  
 398 We allowed the sensor to be stationary and on all the time, negating the trigger-  
 399 ing, and time expansion issues that could exist in real life. In the simulation we

ran the speed of the animal as  $40 \text{ km days}^{-1}$ , the largest day range of terrestrial animals (Carbone *et al.*, 2005). Other speed values should not alter the accuracy of the gREM (precision would be affected, all else being equal, since slower speeds produce fewer records). We also assume perfect knowledge of the average speed of an animal and size of the detection zone, and instant triggering of the camera. All of which may lead to possible bias or a decrease in precision.

**Implications for conservation.** The gREM is available for the estimation of density of a number of taxa where no, or few, accurate methods currently exist to measure absolute animal density (Thomas & Marques, 2012). The species that can now be studied may be of importance to conservation, for example current methods of density estimation for the threatened Franciscana dolphin may result in underestimation of numbers (Crespo *et al.*, 2010). This new method may be important for the study of zoonotic diseases, for example estimating population sizes of bats, which are important reservoir of infectious disease that affect humans, livestock and wildlife (Calisher *et al.*, 2006). In addition, the gREM will make it possible to measure the density of animals which may be useful in quantifying ecosystem services, such as studying the levels of songbirds which are known to have a positive influence on pest control in coffee production (Jirinec *et al.*, 2011). The gREM is suitable for any species that would be consistently recorded within range of a detector, such as bats (Kunz *et al.*, 2009), songbirds (Buckland & Handel, 2006), whales (Marques *et al.*, 2009) or forest primates (Hassel-Finnegan *et al.*, 2008). With increasing technological capabilities, this list of species is likely to increase dramatically.

Importantly the camera trapping and acoustic recording that the gREM use are noninvasive and do not require individual marking (Jewell, 2013) or naturally identifying marks (as required for mark-recapture models). This makes them suitable for large, continuous monitoring projects with limited human resources (Kelly *et al.*, 2012). It also makes them suitable for species that are under pressure, species that cannot naturally be individually recognised or species that are difficult or dangerous to catch (Thomas & Marques, 2012).

1. ACKNOWLEDGMENTS

REFERENCES

- Acevedo, M.A. & Villanueva-Rivera, L.J. (2006) Using automated digital recording systems as effective tools for the monitoring of birds and amphibians. *Wildlife Society Bulletin*, **34**, 211–214.
- Ahlen, I. & Baagøe, H.J. (1999) Use of ultrasound detectors for bat studies in europe: experiences from field identification, surveys, and monitoring. *Acta Chiropterologica*, **1**, 137–150.
- Anderson, D.R. (2001) The need to get the basics right in wildlife field studies. *Wildlife Society Bulletin*, pp. 1294–1297.
- Barlow, J. & Taylor, B. (2005) Estimates of sperm whale abundance in the north-eastern temperate pacific from a combined acoustic and visual survey. *Marine Mammal Science*, **21**, 429–445.
- Blumstein, D.T., Mennill, D.J., Clemins, P., Girod, L., Yao, K., Patricelli, G., Deppe, J.L., Krakauer, A.H., Clark, C., Cortopassi, K.A. *et al.* (2011) Acoustic monitoring in terrestrial environments using microphone arrays: applications, technological considerations and prospectus. *Journal of Applied Ecology*, **48**, 758–767.
- Brusa, A. & Bunker, D.E. (2014) Increasing the precision of canopy closure estimates from hemispherical photography: Blue channel analysis and under-exposure. *Agricultural and Forest Meteorology*, **195**, 102–107.
- Buckland, S.T. & Handel, C. (2006) Point-transect surveys for songbirds: robust methodologies. *The Auk*, **123**, 345–357.
- Buckland, S.T., Marsden, S.J. & Green, R.E. (2008) Estimating bird abundance: making methods work. *Bird Conservation International*, **18**, S91–S108.
- Calisher, C., Childs, J., Field, H., Holmes, K. & Schountz, T. (2006) Bats: important reservoir hosts of emerging viruses. *Clinical microbiology reviews*, **19**, 531–545.
- Carbone, C., Cowlshaw, G., Isaac, N.J. & Rowcliffe, J.M. (2005) How far do animals go? Determinants of day range in mammals. *The American Naturalist*, **165**, 290–297.
- Clark, C.W. (1995) Application of US Navy underwater hydrophone arrays for scientific research on whales. *Reports of the International Whaling Commission*, **45**,



- 210–212.
- Clement, M.J. & Castleberry, S.B. (2013) Estimating density of a forest-dwelling bat: a predictive model for rafinesque’s big-eared bat. *Population Ecology*, **55**, 205–215.
- Crespo, E.A., Pedraza, S.N., Grandi, M.F., Dans, S.L. & Garaffo, G.V. (2010) Abundance and distribution of endangered franciscana dolphins in argentine waters and conservation implications. *Marine Mammal Science*, **26**, 17–35.
- Cutler, T.L. & Swann, D.E. (1999) Using remote photography in wildlife ecology: a review. *Wildlife Society Bulletin*, pp. 571–581.
- Damuth, J. (1981) Population density and body size in mammals. *Nature*, **290**, 699–700.
- Depraetere, M., Pavoine, S., Jiguet, F., Gasc, A., Duvail, S. & Sueur, J. (2012) Monitoring animal diversity using acoustic indices: implementation in a temperate woodland. *Ecological Indicators*, **13**, 46–54.
- Elphick, C.S. (2008) How you count counts: the importance of methods research in applied ecology. *Journal of Applied Ecology*, **45**, 1313–1320.
- Everatt, K.T., Andresen, L. & Somers, M.J. (2014) Trophic scaling and occupancy analysis reveals a lion population limited by top-down anthropogenic pressure in the limpopo national park, mozambique. *PloS one*, **9**, e99389.
- Foster, R.J. & Harmsen, B.J. (2012) A critique of density estimation from camera-trap data. *The Journal of Wildlife Management*, **76**, 224–236.
- Harris, D., Matias, L., Thomas, L., Harwood, J. & Geissler, W.H. (2013) Applying distance sampling to fin whale calls recorded by single seismic instruments in the northeast atlantic. *The Journal of the Acoustical Society of America*, **134**, 3522–3535.
- Hassel-Finnegan, H.M., Borries, C., Larney, E., Umponjan, M. & Koenig, A. (2008) How reliable are density estimates for diurnal primates? *International Journal of Primatology*, **29**, 1175–1187.
- Hutchinson, J.M.C. & Waser, P.M. (2007) Use, misuse and extensions of “ideal gas” models of animal encounter. *Biological Reviews of the Cambridge Philosophical Society*, **82**, 335–359.

- 492 Jewell, Z. (2013) Effect of monitoring technique on quality of conservation science.  
493 *Conservation Biology*, **27**, 501–508.
- 494 Jirinec, V., Campos, B.R. & Johnson, M.D. (2011) Roosting behaviour of a migratory  
495 songbird on jamaican coffee farms: landscape composition may affect delivery  
496 of an ecosystem service. *Bird Conservation International*, **21**, 353–361.
- 497 Jones, K.E., Bielby, J., Cardillo, M., Fritz, S.A., O'Dell, J., Orme, C.D.L., Safi, K.,  
498 Sechrest, W., Boakes, E.H., Carbone, C. *et al.* (2009) PanTHERIA: a species-level  
499 database of life history, ecology, and geography of extant and recently extinct  
500 mammals: Ecological archives e090-184. *Ecology*, **90**, 2648–2648.
- 501 Karanth, K. (1995) Estimating tiger (*Panthera tigris*) populations from camera-trap  
502 data using capture–recapture models. *Biological Conservation*, **71**, 333–338.
- 503 Kelly, M.J., Betsch, J., Wultsch, C., Mesa, B. & Mills, L.S. (2012) Noninvasive sam-  
504 pling for carnivores. *Carnivore ecology and conservation: a handbook of techniques*  
505 (*L Boitani and RA Powell, eds*) Oxford University Press, New York, pp. 47–69.
- 506 Kessel, S., Cooke, S., Heupel, M., Hussey, N., Simpfendorfer, C., Vagle, S. & Fisk, A.  
507 (2014) A review of detection range testing in aquatic passive acoustic telemetry  
508 studies. *Reviews in Fish Biology and Fisheries*, **24**, 199–218.
- 509 Kimura, S., Akamatsu, T., Dong, L., Wang, K., Wang, D., Shibata, Y. & Arai, N.  
510 (2014) Acoustic capture-recapture method for towed acoustic surveys of echolo-  
511 cating porpoises. *The Journal of the Acoustical Society of America*, **135**, 3364–3370.
- 512 Kunz, T.H., Betke, M., Hristov, N.I. & Vonhof, M. (2009) Methods for assessing  
513 colony size, population size, and relative abundance of bats. *Ecological and be-*  
514 *havioral methods for the study of bats* (*TH Kunz and S Parsons, eds*) 2nd ed Johns  
515 Hopkins University Press, Baltimore, Maryland, pp. 133–157.
- 516 Lammers, M.O. & Au, W.W. (2003) Directionality in the whistles of hawaiian spin-  
517 ner dolphins (*stenella longirostris*): A signal feature to cue direction of move-  
518 ment? *Marine Mammal Science*, **19**, 249–264.
- 519 Lewis, T., Gillespie, D., Lacey, C., Matthews, J., Danbolt, M., Leaper, R.,  
520 McLanaghan, R. & Moscrop, A. (2007) Sperm whale abundance estimates from  
521 acoustic surveys of the ionian sea and straits of sicily in 2003. *Journal of the Ma-*  
522 *rine Biological Association of the United Kingdom*, **87**, 353–357.

- Manzo, E., Bartolommei, P., Rowcliffe, J.M. & Cozzolino, R. (2012) Estimation of population density of european pine marten in central italy using camera trapping. *Acta Theriologica*, **57**, 165–172.
- Marcoux, M., Auger-Méthé, M., Chmelnitsky, E.G., Ferguson, S.H. & Humphries, M.M. (2011) Local passive acoustic monitoring of narwhal presence in the canadian arctic: a pilot project. *Arctic*, pp. 307–316.
- Marques, T.A., Munger, L., Thomas, L., Wiggins, S. & Hildebrand, J.A. (2011) Estimating North Pacific right whale (*Eubalaena japonica*) density using passive acoustic cue counting. *Endangered Species Research*, **13**, 163–172.
- Marques, T.A., Thomas, L., Ward, J., DiMarzio, N. & Tyack, P.L. (2009) Estimating cetacean population density using fixed passive acoustic sensors: An example with Blainville’s beaked whales. *The Journal of the Acoustical Society of America*, **125**, 1982–1994.
- O’Brien, T.G., Kinnaird, M.F. & Wibisono, H.T. (2003) Crouching tigers, hidden prey: Sumatran tiger and prey populations in a tropical forest landscape. *Animal Conservation*, **6**, 131–139.
- O’Farrell, M.J. & Gannon, W.L. (1999) A comparison of acoustic versus capture techniques for the inventory of bats. *Journal of Mammalogy*, pp. 24–30.
- Proctor, M., McLellan, B., Boulanger, J., Apps, C., Stenhouse, G., Paetkau, D. & Mowat, G. (2010) Ecological investigations of grizzly bears in canada using dna from hair, 1995-2005: a review of methods and progress. *Ursus*, **21**, 169–188.
- Purvis, A., Gittleman, J.L., Cowlshaw, G. & Mace, G.M. (2000) Predicting extinction risk in declining species. *Proceedings of the Royal Society of London Series B: Biological Sciences*, **267**, 1947–1952.
- R Development Core Team (2010) *R: A Language And Environment For Statistical Computing*. R Foundation For Statistical Computing, Vienna, Austria. ISBN 3-900051-07-0.
- Richter-Dyn, N. & Goel, N.S. (1972) On the extinction of a colonizing species. *Theoretical Population Biology*, **3**, 406–433.
- Rogers, T.L., Ciaglia, M.B., Klinck, H. & Southwell, C. (2013) Density can be misleading for low-density species: benefits of passive acoustic monitoring. *Public Library of Science One*, **8**, e52542.

- 555 Rovero, F., Zimmermann, F., Berzi, D. & Meek, P. (2013) " which camera trap type  
556 and how many do i need?" a review of camera features and study designs for a  
557 range of wildlife research applications. *Hystrix*.
- 558 Rowcliffe, J.M. & Carbone, C. (2008) Surveys using camera traps: are we looking  
559 to a brighter future? *Animal Conservation*, **11**, 185–186.
- 560 Rowcliffe, J., Field, J., Turvey, S. & Carbone, C. (2008) Estimating animal density  
561 using camera traps without the need for individual recognition. *Journal of Ap-  
562 plied Ecology*, **45**, 1228–1236.
- 563 Schmidt, B.R. (2003) Count data, detection probabilities, and the demography, dy-  
564 namics, distribution, and decline of amphibians. *Comptes Rendus Biologies*, **326**,  
565 119–124.
- 566 Smouse, P.E., Focardi, S., Moorcroft, P.R., Kie, J.G., Forester, J.D. & Morales, J.M.  
567 (2010) Stochastic modelling of animal movement. *Philosophical Transactions of the  
568 Royal Society B: Biological Sciences*, **365**, 2201–2211.
- 569 Soisalo, M.K. & Cavalcanti, S. (2006) Estimating the density of a jaguar population  
570 in the Brazilian Pantanal using camera-traps and capture-recapture sampling in  
571 combination with GPS radio-telemetry. *Biological Conservation*, **129**, 487–496.
- 572 Sollmann, R., Gardner, B., Chandler, R.B., Shindle, D.B., Onorato, D.P., Royle, J.A.  
573 & O’Connell, A.F. (2013) Using multiple data sources provides density estimates  
574 for endangered florida panther. *Journal of Applied Ecology*, **50**, 961–968.
- 575 SymPy Development Team (2014) *SymPy: Python library for symbolic mathematics*.
- 576 Thomas, L. & Marques, T.A. (2012) Passive acoustic monitoring for estimating an-  
577 imal density. *Acoustics Today*, **8**, 35–44.
- 578 Trolle, M. & Kéry, M. (2003) Estimation of ocelot density in the Pantanal using  
579 capture-recapture analysis of camera-trapping data. *Journal of mammalogy*, **84**,  
580 607–614.
- 581 Trolle, M., Noss, A.J., Lima, E.D.S. & Dalponte, J.C. (2007) Camera-trap studies of  
582 maned wolf density in the Cerrado and the Pantanal of Brazil. *Biodiversity and  
583 Conservation*, **16**, 1197–1204.
- 584 Walters, C.L., Collen, A., Lucas, T.C.D., Mroz, K., Sayer, C.A. & Jones, K.E. (2013)  
585 Challenges of using bioacoustics to globally monitor bats. *Bat Evolution, Ecology,  
586 and Conservation*, pp. 479–499. Springer.

- 587 Wright, S.J. & Hubbell, S.P. (1983) Stochastic extinction and reserve size: a focal  
588 species approach. *Oikos*, pp. 466–476.
- 589 Yapp, W. (1956) The theory of line transects. *Bird study*, **3**, 93–104.
- 590 Zero, V.H., Sundaresan, S.R., O'Brien, T.G. & Kinnaird, M.F. (2013) Monitoring  
591 an endangered savannah ungulate, Grevy's zebra (*Equus grevyi*): choosing a  
592 method for estimating population densities. *Oryx*, **47**, 410–419.

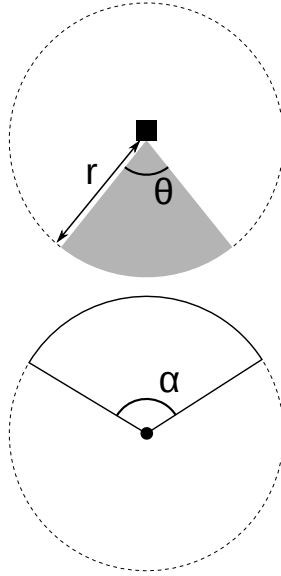


FIGURE 1. Representation of sensor detection width and animal signal width. The filled square and circle represent a sensor and an animal, respectively;  $\theta$ , sensor detection width (radians);  $r$ , sensor detection distance; dark grey shaded area, sensor detection zone;  $\alpha$ , animal signal width (radians). Dashed lines around the filled square and circle represents the maximum extent of  $\theta$  and  $\alpha$ , respectively.

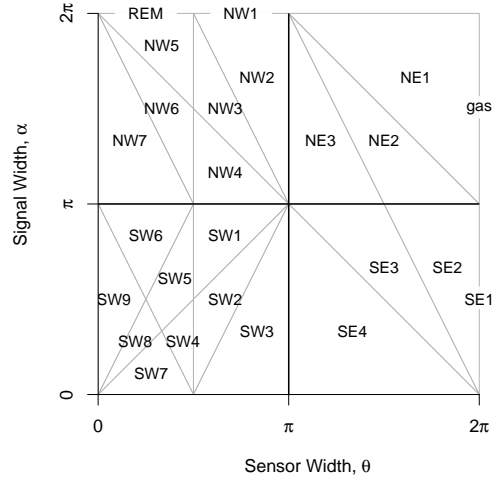


FIGURE 2. Locations where derivation of the average profile  $\bar{p}$  is the same for different combinations of sensor detection width and animal signal width. Symbols within each polygon refer to each gREM submodel named after their compass point, except for Gas and REM which highlight the position of these previously derived models within the gREM. Symbols on the edge of the plot are for submodels with  $\alpha, \theta = 2\pi$

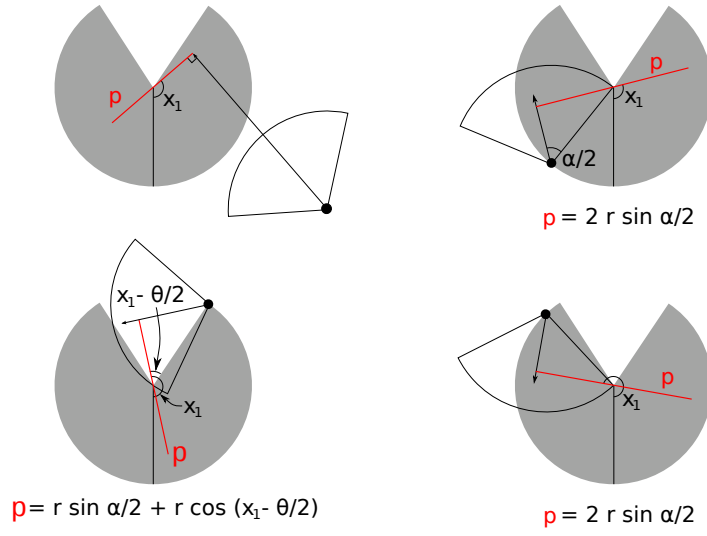


FIGURE 3. An overview of the derivation of SE2. The filled circles represent animals, with the animal signal shown as a unfilled sector and the direction of movement shown as an arrow. The detection zone of the sensor is shown as filled grey sectors with a detection distance of  $r$ . The vertical black line within the circle shows the direction the sensor is facing;  $\theta$ , sensor detection width;  $\alpha$ , animal signal width. The profile  $p$  (the line an animal must pass through in order to be captured) is shown in red and  $x_1$  is the focal angle, where (a) shows the location of  $x_1$ . The derivation of  $p$  changes as the animal approaches the sensor from different directions where (b) is the derivation of  $p$  when  $x_1$  is in the interval  $[\frac{\pi}{2}, \frac{\pi}{2} + \frac{\theta}{2} - \frac{\alpha}{2}]$ , (c)  $p$  when  $x_1$  is in the interval  $[\frac{\pi}{2} + \frac{\theta}{2} - \frac{\alpha}{2}, \frac{5\pi}{2} - \frac{\theta}{2} - \frac{\alpha}{2}]$  and (d)  $p$  when  $x_1$  is in the interval  $[\frac{5\pi}{2} - \frac{\theta}{2} - \frac{\alpha}{2}, \frac{3\pi}{2}]$ . The resultant equation for  $p$  is shown beneath each figure.



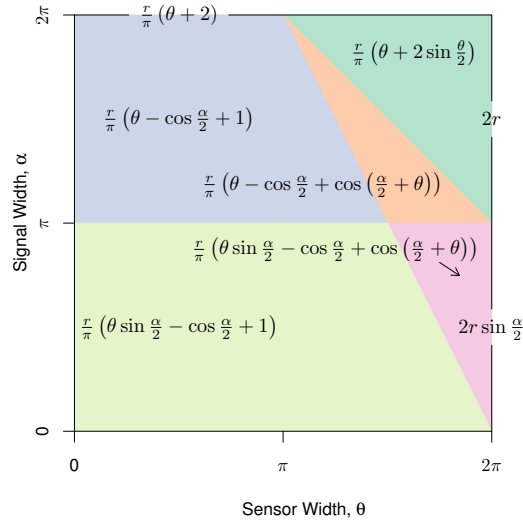


FIGURE 4. Expressions for the average profile width,  $\bar{p}$ , given sensor and signal widths. Despite independent derivation within each block, many models result in the same expression. These are collected together and presented as one block of colour. Expressions on the edge of the plot are for submodels with  $\alpha, \theta = 2\pi$ .

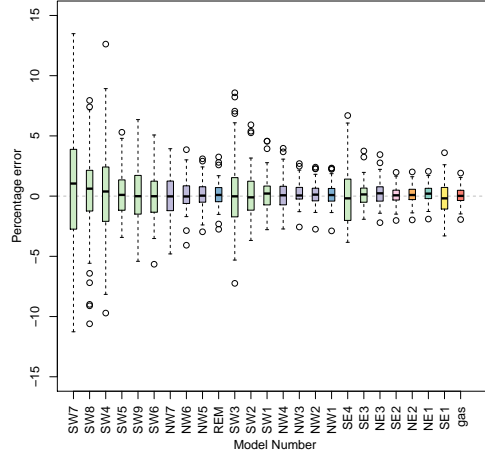


FIGURE 5. Simulation model results of the accuracy and precision for gREM submodels. The percentage error between estimated and true density for each gREM submodel is shown within each box plot, where the black line represents the median percentage error across all simulations, boxes represent the the middle 50% of the data, whiskers represent variability outside the upper and lower quartiles with outliers plotted as individual points. Box colours correspond to the expressions for average profile width  $\bar{p}$  given in Figure 4.

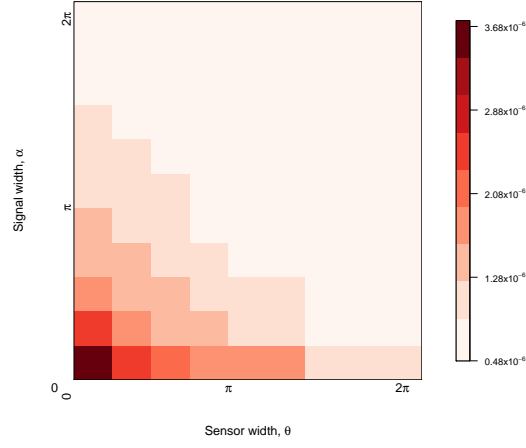


FIGURE 6. Simulation model results of the gREM precision given a range of sensor and signal widths, shown by the standard deviation of the error between the estimated and true densities. Standard deviations are shown from deep red to pink, representing high to low values between  $0.483 \times 10^{-6}$  to  $3.74 \times 10^{-6}$ .

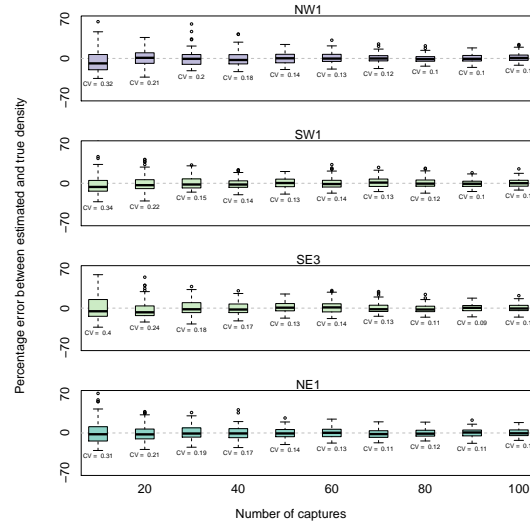
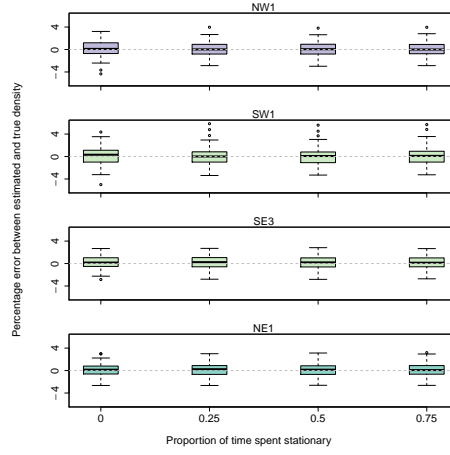
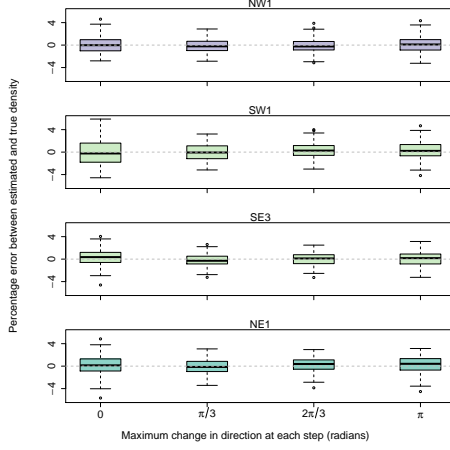


FIGURE 7. Simulation model results of the accuracy and precision of four gREM submodels (NW1, SW1, SE3 and NE1) given different numbers of captures. The percentage error between estimated and true density within each gREM sub model for capture rate is shown within each box plot. Sensor and signal widths vary between submodels. The number beneath each plot represents the coefficient of variation. The colour of each box plot corresponds to the expressions for average profile width  $\bar{p}$  given in Figure 4.



(A)



(B)

FIGURE 8. Simulation model results of the accuracy and precision of four gREM submodels (NW1, SW1, SE3 and NE1) given different movement models where (A) amount of time spent stationary (stop-start movement) and (B) maximum change in direction at each step (correlated random walk model). The percentage error between estimated and true density within each gREM sub model for the different movement models is shown within each box plot. The simple model is represented where time and maximum change in direction equals 0. The colour of each box plot corresponds to the expressions for average profile width  $\bar{p}$  given in Figure 4.